

Raman Scattering by Optical Phonons in Isotopic $^{70}\text{Ge}_n^{74}\text{Ge}_n$ Superlattices

J. Spitzer, T. Ruf, and M. Cardona

Max-Planck-Institut für Festkörperforschung, Heisenbergstrasse 1, D-70569 Stuttgart, Federal Republic of Germany

W. Dondl, R. Schorer, and G. Abstreiter

Walter-Schottky-Institut, Technische Universität München, Am Coulombwall, D-85748 Garching, Federal Republic of Germany

E. E. Haller

University of California and Lawrence Berkeley Laboratory, Berkeley, California 94720

(Received 29 November 1993)

We present Raman spectra of a series of isotopic $^{70}\text{Ge}_n^{74}\text{Ge}_n$ superlattices with $2 \leq n \leq 32$. In these novel structures only the phonons are subject to a periodic isotopic mass modulation, whereas the electrons retain their bulklike character. This differs substantially from conventional superlattices where both electronic and vibronic properties are affected by the reduction in dimensionality. Our results show clear evidence for optic phonon confinement in each of the two superlattice constituents. Observed frequencies, relative intensities, and mode mixing compare favorably with calculations based on a planar bond-charge model and the bond polarizability approach.

PACS numbers: 78.30.Hv, 68.55.Bd, 68.65.+g, 78.66.Li

The physics of reduced dimensionality in solids is accessible almost exclusively via semiconductor heterostructures. Their investigation by means of electrical and optical methods has not only evolved into one of the most important branches of modern semiconductor physics, but also represents the basis of numerous novel device concepts (see, e.g., Ref. [1], and references therein). Fundamental aspects, such as the effect of the artificial superlattices' (SL's) periodicity on electronic and vibrational properties, have been investigated by Raman spectroscopy [2]. Most of these studies have been concerned with GaAs/AlAs SL's due to the high technological standards which have been achieved in growing this particular material combination [3]. Although GaAs/AlAs SL's exhibit no strain effects due to lattice mismatch, in contrast to, e.g., those made of Si and Ge [4], the reduction in dimensionality still changes both electronic *and* vibronic properties dramatically. This prevents the distinction and separate treatment of both effects. Only very recently the prospect of decoupling these two effects has been opened by the availability of isotopically pure germanium [5,6]. Natural Ge consists of five stable isotopes (21.2% ^{70}Ge , 27.7% ^{72}Ge , 7.7% ^{73}Ge , 35.9% ^{74}Ge , and 7.4% ^{76}Ge) and isotopically pure crystals have been so far mainly used to study effects of isotopic disorder on vibrational spectra [7-10].

In this work we report Raman measurements on a novel kind of heterostructure, a series of isotopic $^{70}\text{Ge}_n^{74}\text{Ge}_n$ SL's. These samples represent an excellent model system to study the vibronic properties of SL's because the electronic structure should be affected only weakly by changes in the isotopic mass. Since these changes are the only difference between the SL constituents, Raman spectroscopy is the only non-destructive method to investigate their structural prop-

erties. Experimental data are compared with the results of a planar force-constant model [11]. Our data show clear evidence for confinement of the optical phonons in the two different materials and disorder-induced features (so-called band modes) which are attributed to intermixing of the two isotopes at the layer interfaces.

The samples were grown by molecular beam epitaxy (MBE) on nominally intrinsic Ge [001] substrates. On top of the substrate a ^{70}Ge buffer layer with a thickness of 230 Å was deposited to prepare an atomically smooth surface. The $^{70}\text{Ge}_n^{74}\text{Ge}_n$ SL's were grown on this buffer at a temperature of 350 °C and low growth rates of 4 Å/min from standard PBN-Knudsen cells. The overall thickness of the SL's is about 400 monolayers (ML) (1 ML = 1.41 Å) with single layer thicknesses $n=2, 4, 6, 8, 12, 16,$ and 32 ML. For comparison with previous Raman results [9] a $(^{70}\text{Ge})_{0.5}({}^{74}\text{Ge})_{0.5}$ alloy and pure ^{70}Ge and ^{74}Ge samples were grown as well.

Raman spectra were recorded in backscattering geometry using the lines of Ar⁺ and Kr⁺ lasers. The collected light was dispersed by a 0.85 m SPEX double monochromator and detected with conventional single photon counting. The spectral resolution was 1 cm⁻¹, as determined by direct measurement of the laser line. To investigate the disorder-induced band modes of the samples we used a DILOR XY triple monochromator and accumulated the signal with a charged coupled device multichannel detection system. The samples were kept in a closed-cycle cryostat at a temperature of 10 K.

Figure 1 summarizes the experimental data and the results of our calculations. The former, shown in Fig. 1(a), clearly exhibit an increasing number of modes with increasing SL period. These modes can be identified as optical phonons fully or partly confined in the two different constituents of the SL's. The occurrence of confined

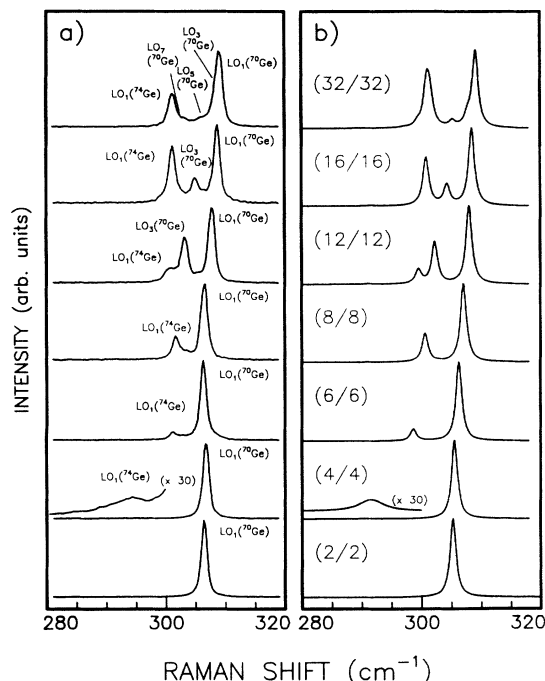


FIG. 1. (a) Measured and (b) calculated Raman spectra for a series of isotopic ⁷⁰Ge_{n⁷⁴Ge_{n SL's showing various confined modes of ⁷⁰Ge and ⁷⁴Ge layers. The measurements were performed with the 514.5 nm line of an Ar⁺-ion laser at a temperature of 10 K. Calculated Raman peaks have been numerically broadened by 1.2 cm⁻¹ to facilitate comparison with experiment.}}

optical modes is somewhat surprising since the phonon dispersions of ⁷⁰Ge and ⁷⁴Ge overlap over a large frequency range. As will be discussed later, the assignment of these modes to confined SL phonons is possible by comparison with our calculations. The labels LO_n(⁷⁰Ge) and LO_n(⁷⁴Ge) in Fig. 1(a) denote the material in which the corresponding longitudinal optic (LO_n) mode has the strongest vibrational amplitude. Only modes with odd *n* are Raman active [12].

Calculations were performed in the framework of the planar force-constant model [11], with the electronic degrees of freedom described by a bond charge of zero mass midway between the atomic planes. The inclusion of these bond-charge planes has proven useful to reproduce the flattening of the transverse acoustic (TA) modes at the Brillouin zone edge [13,14]. The force constants used are those obtained in Ref. [12] from fitting the calculated bulk phonon dispersion curves of natural Ge to experimental neutron scattering data [15]. Diagonalization of the dynamical matrix for the SL's yields the eigenvalues (vibrational frequencies) and eigenvectors (displacements) of the vibrational modes. The Raman spectra given in Fig. 1(b) have been calculated from these data using the bond polarizability model [2,16] which requires only one adjustable parameter to describe the overall absolute scattering cross section. Since we did not deter-

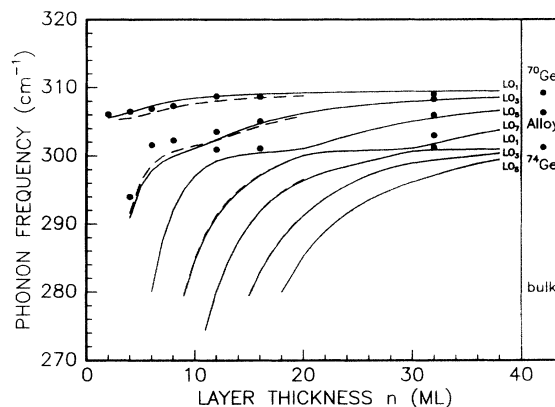


FIG. 2. Measured (dots) and calculated (solid line) confined LO phonon frequencies vs SL layer thickness *n*. The dashed line represents a calculation which considers intermixing at the interface. Note the anticrossings near *n* = 12, 20, 30 which are discussed in the text.

mine absolute cross sections, our calculations are to be regarded as parameter free. To allow better comparison with the experiment [Fig. 1(a)] the calculated Raman lines [Fig. 1(b)] have been broadened by 1.2 cm⁻¹. Experiment and calculation compare favorably and will be discussed in more detail in the following.

In Figs. 2 and 3 we plot measured frequencies (laser energy *E_L* = 2.409 eV) and relative intensities of these modes together with theoretical results vs SL layer thickness *n*. Because of the fact that the planar force-constant model was fitted to natural germanium without removing self-energies due to isotopic disorder [17], and to a small deficiency of the fits for bulk *k* = 0 phonons, the calculated frequencies are about 2 cm⁻¹ higher than the measured ones. Therefore we rigidly shifted the calculated frequencies by 2 cm⁻¹ to lower energies in Fig. 2, using

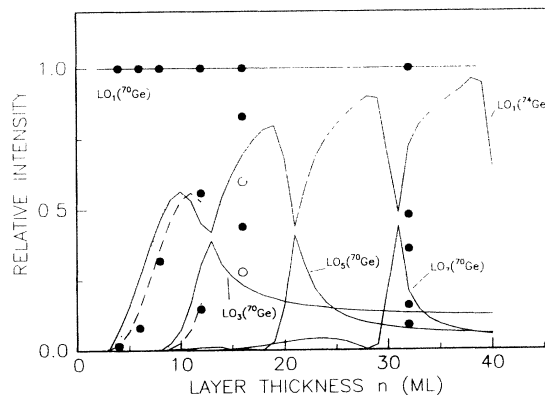


FIG. 3. Measured ($\lambda_L=5145 \text{ \AA}$, \bullet ; $\lambda_L=6471 \text{ \AA}$, \circ) and calculated (lines) relative LO phonon intensities vs SL layer thickness *n*. Solid lines represent calculations for a perfect SL; dashed and dotted lines are calculations which treat intermixing at the interfaces according to two different models. See text for details.

the measured frequencies of the ^{70}Ge and ^{74}Ge samples as reference points. The experimental LO phonon frequencies of these two samples and the $(^{70}\text{Ge})_{0.5}({}^{74}\text{Ge})_{0.5}$ alloy are given, labeled as bulk, at the right edge of the plot. From their energies and the atomic displacement patterns for the different samples (to be published elsewhere, see also Ref. [17]) one can identify the different modes as LO_n predominantly confined phonons in either layer. For small layer thicknesses, however, the experimental frequencies of the $\text{LO}_1({}^{74}\text{Ge})$ mode deviates slightly from theory. Around 12, 20, and 30 ML pronounced anticrossings between different branches of the optical modes occur. At these points confined LO_n modes of ^{70}Ge layers become degenerate with the LO_1 phonon of ^{74}Ge . Since they have the same symmetry, these modes interact and anticrossings appear. This behavior can be observed even better in Fig. 3, where we show the experimental relative intensities, normalized to that of the respective $\text{LO}_1({}^{70}\text{Ge})$ mode for each sample, together with calculated values. The agreement of experimental relative intensities and calculated values can be improved by considering isotopic intermixing at the SL interfaces, which becomes more important for the shorter-period samples. In order to evaluate this intermixing theoretically we used two different models. In the first one we defined an "effective mass" for each layer including two monolayers of a 50% alloy at each interface when calculating the average mass in each layer. The result of this calculation is shown by the dashed lines in Fig. 3. In a second approach we introduced two discrete alloy layers, with average mass atoms at each interface and diagonalized the dynamical matrix of a three-layer supercell. These results are shown as the dotted lines in Fig. 3. Although the first model is the simpler one, as it averages over layers and describes alloying effects at the interface with a modulation of the mass in the whole layer, it appears to give the more adequate description of the observed relative intensities. Especially for the samples with $n = 4, 6,$ and 8 the agreement between measurements and the calculation is substantially improved. However, we consider alloying effects to be important only for the samples with smaller layer thickness and therefore applied these alloy models only up to 12 ML. For the SL with $n = 16$ pronounced differences of measured and calculated values occur. They seem to be related to resonance effects near the E_1 and $E_1 + \Delta_1$ critical points of Ge which lie at 2.2 eV and 2.4 eV, respectively [18]. Preliminary resonant Raman experiments show a dependence of the resonance energy for relative phonon intensities on the SL period. This result is unexpected as the electronic structure, as mentioned above, should be affected only weakly by changes of the isotopic mass. To illustrate the strength of the resonance effect we show in Fig. 3 the off-resonance intensity ratio for the $n = 16$ sample measured with a laser energy of $E_L = 1.916$ eV as open circles. For all other samples the

intensity ratio peaks above 2.5 eV and data taken at this energy can be regarded as nonresonant. To complete the discussion of the influence of interface disorder on the Raman spectra we note that the inclusion of isotopic intermixing has only a small effect on the dependence of calculated frequencies on SL layer thickness (cf. Fig. 2). Calculated frequencies are changed by about 1 cm^{-1} in the alloy model and by about 0.5 cm^{-1} in the three-layer model. The frequency shift of different confined modes, however, is of opposite sign. This describes correctly the trend of the deviations between experiment and calculation and is shown for the alloy model as the dashed lines in Fig. 2.

Figure 4 displays the frequency range below the main Raman lines discussed in Fig. 1 for the whole series of SL's. In this region the bulk density of states has its maximum [9], leading, in the presence of isotopic disorder, to so-called *band modes*. This has been investigated in detail in bulk isotopic Ge [9]. In the case of a perfect isotopic SL with no intermixing at the interfaces these band modes should be replaced by higher order confined LO modes lying in this frequency range. In real isotopic SL's, however, intermixing exists at the interfaces. Therefore any mode in this frequency range has to be regarded as the sum of an "alloy part" (band modes) and a "SL part" (higher order confined LO). In order to compare the experiment with our calculations we first subtracted the stronger LO modes (shown in Fig. 1), represented by Lorentzians and after normalizing the highest one to unity. From the remaining part of the spectra we then subtracted the alloy part [9] which was taken to

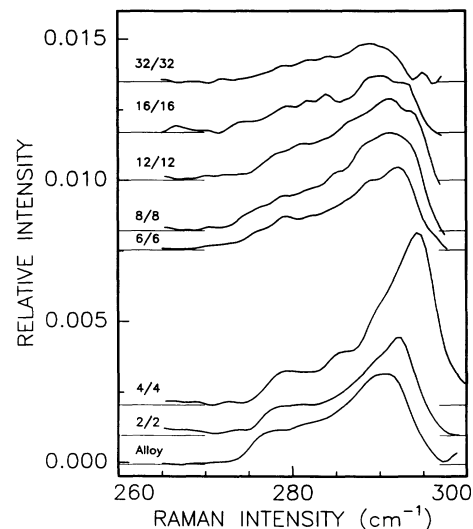


FIG. 4. Raman spectra in the energy range of vibrational band modes in isotopic SL's. The data were obtained by subtracting the tail of the main Raman line(s) from the original data in Fig. 1. The intensities are normalized to that of the respective $\text{LO}_1({}^{70}\text{Ge})$ phonon. The spectra were vertically shifted for clarity. See text for details.

TABLE I. Measured and calculated strength of the "SL part" of the band modes of Fig. 4. The values in parentheses give the calculations for 9/7 instead of 8/8 ML and 7/5 instead of 6/6 ML.

SL period	"SL part"	
	Measured	Calculated
4	0.03	0.05
6	0.02	0.0003 (0.003)
8	0.03	0.008 (0.03)
12	0.03	0.03
16	0.02	0.02
32	0.01	0.01

correspond to 2 ML per SL layer. Figure 4 displays the pure SL part of the isotopic SL's so obtained. In Table I we compare the integrated intensities of these SL parts with the calculated ones obtained by integrating the higher order LO modes of the SL's. Calculated and measured strengths compare favorably for most of the samples. Only in the case of $n = 6$ and $n = 8$ is the calculated SL part too small. For the $n = 8$ SL this problem can be overcome by considering a 9/7 ML period, which leads to a strength in agreement with the experimental value (given in brackets in Table I). This is not the case for the $n = 6$ SL, where even a period of 7/5 ML yields a much too small value (also given in brackets in Table I).

In conclusion, we have presented Raman spectra of a series of isotopic $^{70}\text{Ge}_n^{74}\text{Ge}_n$ SL's. These samples represent an excellent model system for the investigation of confinement of optical phonons in SL's. Both frequencies and relative intensities of the measured spectra are in good agreement with calculations based on a planar bond-charge model and the bond-polarizability approach. From the comparison of experiment and theory we were able to show that intermixing of the two isotopes at the interfaces occurs but is limited to 1 ML in each direction. This intermixing was also found to be responsible for the observation of disorder-induced band modes whose intensity decreases with increasing SL period. The high quality of these SL's may make them suitable for electronic applications through neutron transmutation [19].

We thank P. Molinàs-Mata for help with the planar bond-charge model and H. Hirt, M. Siemers, and P. Wurster for technical support. The work at the

Walter Schottky Institut was financially supported by Stiftung Volkswagenwerk and ESPRIT Basic Research Project P 7128. E.E.H. was supported in part by the Laboratory Direct Research and Development Program of the Lawrence Berkeley Laboratory through the U.S. Department of Energy under Contract No. DE-AC03-76SF00098.

- [1] C. Weisbuch and B. Vinter, *Quantum Semiconductor Structures* (Academic Press, San Diego, 1991).
- [2] B. Jusserand and M. Cardona, in *Light Scattering in Solids*, edited by M. Cardona and G. Güntherodt (Springer, Heidelberg, 1989), Vol. V, p. 49.
- [3] K. Ploog, *Angew. Chem. Int. Ed. Engl.* **27**, 593 (1988).
- [4] J.C. Bean, in *Silicon-Molecular Beam Epitaxy*, edited by E. Kasper and J.C. Bean (CRC Press, Boca Raton, FL, 1988), p. 65.
- [5] V.F. Agekyan, V.M. Asnin, A.M. Kryukov, I.I. Markov, N.A. Rud, V.I. Stepanov, and A.B. Churilov, *Fiz. Tverd. Tela (Leningrad)* **31**, 101 (1989) [*Sov. Phys. Solid State* **31**, 2082 (1989)].
- [6] K. Itoh, W.L. Hansen, E.E. Haller, J.W. Farmer, V.I. Ozhogin, A. Rudnev, and A. Tikhomirov, *J. Mater. Res.* **8**, 1341 (1993).
- [7] H.D. Fuchs, C.H. Grein, C. Thomsen, M. Cardona, W.L. Hansen, E.E. Haller, and K. Itoh, *Phys. Rev. B* **43**, 4835 (1991).
- [8] H.D. Fuchs, C.H. Grein, M. Bauer, and M. Cardona, *Phys. Rev. B* **45**, 4065 (1992).
- [9] H.D. Fuchs, P. Etchegoin, M. Cardona, K. Itoh, and E.E. Haller, *Phys. Rev. Lett.* **70**, 1715 (1993).
- [10] H.D. Fuchs, Ph.D. thesis, Stuttgart, 1993.
- [11] P. Molinàs-Mata and M. Cardona, *Phys. Rev. B* **43**, 9799 (1991).
- [12] M. Cardona, in *Light Scattering in Solids*, edited by M. Cardona and G. Güntherodt (Springer, Heidelberg, 1989), Vol. II, p. 14.
- [13] P. Molinàs i Mata, M.I. Alonso, and M. Cardona, *Solid State Commun.* **74**, 347 (1990).
- [14] P. Molinàs-Mata, A.J. Shields, and M. Cardona, *Phys. Rev. B* **47**, 1866 (1993).
- [15] G. Nilsson and G. Nelin, *Phys. Rev. B* **3**, 364 (1971).
- [16] H.D. Fuchs, P. Molinàs-Mata, and M. Cardona, *Superlattices Microstruct.* **13**, 447 (1993).
- [17] P. Etchegoin, H.D. Fuchs, J. Weber, M. Cardona, L. Pintschovius, N. Pyka, K. Itoh, and E.E. Haller, *Phys. Rev. B* **48**, 12661 (1993).
- [18] M.I. Alonso and M. Cardona, *Phys. Rev. B* **37**, 10107 (1988).
- [19] E.E. Haller, *Semicond. Sci. Technol.* **5**, 319 (1990).